PHYSICAL REVIEW B VOLUME 35, NUMBER 3 15 JANUARY 1987-II

Phenomenological theory of optical second- and third-harmonic generation from cubic centrosymmetric crystals

J. E. Sipe, D. J. Moss, and H. M. van Driel
Department of Physics, and Erindale College, University of Toronto, Toronto, Ontario, Canada M5S 1A7
(Received 21 August 1986)

We present a macroscopic theory for anisotropic second- and third-harmonic generation obtained in reflection from the surface and bulk of cubic centrosymmetric single crystals. The theory is based on possible electric dipole, electric quadrupole, and magnetic dipole sources. Completely general expressions for the harmonic fields are obtained for (100), (111), and (110) faces independent of the details of the surface response but consistent with crystal symmetry. The results obtained agree with all existing experimental data obtained by various groups during the past few years. The possibility of separating out surface and bulk responses is considered using symmetry, polarization, or geometry arguments and it is concluded that for second-harmonic generation this cannot be done in general without additional information. Third-harmonic generation, barring any strong resonantly enhanced surface electric dipole effects, is essentially a bulk probe.

I. INTRODUCTION

In the last few years there has been a resurgence of interest in second- (SHG) and third- (THG) harmonic generation from crystals, in particular, from semiconductors and metals which are cubic and centrosymmetric. Part of this interest was stimulated by the work of Guidotti *et al.*,[1] who noted that the second-harmonic intensity from Ge and Si single crystals displayed a dependence on crystal face and sample orientation. In extensive work on second-harmonic generation almost twenty years ago[2,3] this anisotropy was apparently never observed. Another source for the recent interest is related to the use of nonlinear optical techniques as probes of surface structure and the properties of adsorbed molecules[4,5] or as probes of the bulk structure.[6–10]

In general, in crystals of cubic symmetry the linear optical susceptibility is isotropic in character, whereas the second- and third-order nonlinear susceptibilities, because of their higher tensorial rank, are not. It is this characteristic which has led to the use of nonlinear optical techniques as probes of anisotropic bulk and surface properties. The techniques, particularly SHG, must be used with caution in centrosymmetric media. If one considers SHG, in the bulk of centrosymmetric materials the second-order dipole response ($\chi^{(2)}$) is zero, and so the lowest-order nonlinear response arises from higher-order nonlocal sources with electric quadrupole or magnetic dipole symmetry. At the surface, however, the inversion symmetry is broken and a second-order dipole response can exist. This contribution to SHG arises from a layer a few angstroms thick instead of the entire region within the escape depth of the second-harmonic radiation, as in bulk-originating contributions. The result is that in centrosymmetric crystals, the surface and bulk contributions can be comparable. In some experiments, samples can be prepared in such a way as to enhance the surface contribution so that it can actually dominate the bulk contribution. Indeed, this has been the primary motivating factor for the use of optical SHG as a surface of adsorbates on surfaces,[4] or intrinsic surface reconstruction[5] for cleaved samples in a vacuum. In general, however, for cubic centrosymmetric materials it is not possible to separate out surface and bulk effects, as this paper will show.

In the case of third-harmonic generation, which is electric dipole allowed in the bulk for centrosymmetric materials, the bulk contribution tends to dominate the surface contribution by d/a where d is the escape depth of radiation at the third-harmonic frequency or the coherence length, whichever is shorter and a is the lattice constant. The factor d/a is a measure of the relative number of contributing layers for the bulk and surface contributions. Optical THG is therefore an unambiguous method of probing bulk centrosymmetric crystal properties. Indeed, optical THG has been used[8–10] as such, whereas some controversy has existed[1,6,7] over the source and anisotropy of SHG from cubic crystals.

In order for nonlinear optical techniques to be useful as bulk or surface probes, a macroscopic theory relating the harmonic generation efficiency to the linear and nonlinear response coefficients in the material is needed. Although these coefficients must be calculated in detail from a microscopic theory, the form that they take is restricted by crystal symmetry and is thus dependent on crystal orientation. Phenomenological theories were developed in the 1960s for SHG in cubic[2] and isotropic media.[3] In particular, the theory for cubic media did not explicitly consider anisotropic SHG, in compliance with existing data at the time. However, the more recent observations of anisotropic SHG in semiconductors[1,6,7] and metals[11] have demonstrated a need for a more general theory. Recently, Guyot-Sionnest, Chen, and Shen[12] presented a macroscopic theory for SHG from isotropic materials, and briefly discussed cubic materials. The primary motivation in that paper was to estimate the relative size of the contributions from the bulk and surface of centrosymmetric materials. In order to do this the authors employed a specific model, initially considered by Bloembergen

et al.,[2] for the nonlocal part of the surface response. Their model does offer physical insight into the origins of the surface response, and allows a rough quantitative estimate of the relative size of the surface and bulk response. However, as pointed out by the authors, this model experiences difficulties in that it depends on microscopic variations in the normal component fields and the material properties near the surface, which are mathematically ambiguous. We feel, therefore, that it is useful to present a macroscopic theory for SHG which makes no assumptions about the microscopic physical origins of the surface or bulk response tensor, and instead assumes only a particular macroscopic symmetry (for the surface and bulk). For completeness and comparison, we offer a similar phenomenological theory for bulk THG.

In this paper, we derive the macroscopic phenomenological equations for both SHG and THG obtained in reflection from cubic, centrosymmetric materials. We investigate the possibilities of distinguishing between the surface and bulk responses without introducing a specific surface model. In Sec. II the theory for SHG in reflection from the bulk and surface of centrosymmetric crystals is developed; in Sec. III the macroscopic theory for optical THG is derived for centrosymmetric crystals. The expressions for both SHG and THG are calculated for (111), (110), and (001) crystal faces. Finally the results are analyzed in terms of the symmetry and relative importance for the surface and bulk contributions, and the information that can be obtained about either.

II. THEORY FOR SECOND-HARMONIC GENERATION FROM CENTROSYMMETRIC CUBIC CRYSTALS

A. Bulk contribution

In this section we calculate the reflected second-harmonic fields, generated by a single plane-wave incident on a cubic crystal face with (111), (110), or (001) orientations. The form of the nonlinear response tensor is examined and transformed from the usual crystal coordinate axes to the beam coordinate axes. We then express the nonlinear polarization in the medium in terms of the incident fundamental fields. Finally a Green-function formalism[13] is employed to calculate the resulting external generated fields from the bulk nonlinear polarization.

In the bulk of crystals possessing a center of symmetry, the second-order dipole response, $\vec{\chi}^{(2)} \equiv 0$, and hence the lowest order nonlinear polarization density is of magnetic dipole or electric quadrupole symmetry.[2] In general, this nonlocal response can be written in terms of an effective polarization, as

$$P_i^{(2\omega)}(\mathbf{r}) = \Gamma_{ijkl} E_j^{(\omega)}(\mathbf{r}) \nabla_k E_l^{(\omega)}(\mathbf{r}) , \tag{1}$$

where the gradient is determined with respect to the field coordinates and the summation convention is used. For crystals with bulk cubic symmetry, such as Si or Ge, when the crystal axes are taken to be the standard cubic axes, all distinct elements for a 4th rank tensor are given by

$$\Gamma_{ijkl} = a_1 \delta_{ijkl} + a_2 \delta_{ij}\delta_{kl} + a_3 \delta_{ik}\delta_{jl} + a_4 \delta_{il}\delta_{jk} ,$$

where a_i are constants and $\delta_{ij}\delta_{kl}$ implies $i,j \neq k,l$. Equation (1) can then be written in the usual form[2,6,7,12]

$$P_i^{(2\omega)}(\mathbf{r}) = (\delta - \beta - 2\gamma)(\mathbf{E}\cdot\nabla)E_i + \beta E_i(\nabla\cdot\mathbf{E}) + \gamma \nabla_i(\mathbf{E}\cdot\mathbf{E}) + \zeta E_i \nabla_i E_i , \tag{2}$$

where $\delta,\beta,\gamma,\zeta$ are phenomenological constants and $E_i = E_i^{(\omega)}(\mathbf{r})$ (the frequency dependence of the fundamental field will be suppressed for notational convenience in what follows). The first three terms are isotropic in character while the last is anisotropic with respect to crystal orientation. It may be noted that the last term in Eq. (2) is indeed a vector, since ζ is actually an element of a 4th rank tensor and not a scalar; for different crystal-axis orientations, this term becomes considerably more complex. For excitation of a homogeneous medium by a single transverse plane wave, the first two terms are zero, and the third term generates a polarization which, in an infinite medium, cannot radiate. In a reflection geometry from a finite medium, however, the polarization arising from this term can radiate both into the medium and into the vacuum. For the case of interest here in which we consider the interaction of a single beam with a medium, only the last two terms of Eq. (2) contribute.

Consider then a laser beam, idealized as single incident plane wave at frequency ω and wave vector ν_{0-}, incident on the medium of interest at an angle θ_0 as shown in Fig.

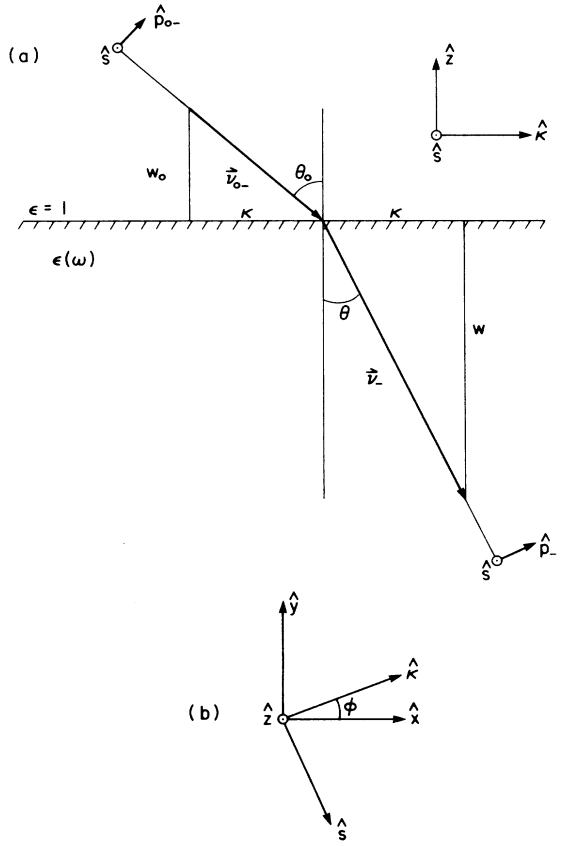

FIG. 1. (a) Geometry and unit vectors for the propagating fundamental fields. Note that the diagram assumes $n = \sqrt{\epsilon(\omega)}$ is real. (b) Beam unit vectors $(\hat{\mathbf{s}},\hat{\boldsymbol{\kappa}})$ in terms of crystal surface unit vectors [given by $\hat{\mathbf{x}}'\hat{\mathbf{y}}'$ in Eqs. (5) and (6)] in the plane of the surface.

1. The incident field can be written as

$$\mathbf{E}_0(\mathbf{r},t)=\mathbf{E}_0 e^{i\boldsymbol{\nu}_{0-}\cdot\mathbf{r}-i\omega t}+\text{c.c.}\ , \tag{3a}$$

where the amplitude can be expressed as a superposition of p- and s-polarized components as

$$\mathbf{E}_0=E_{0p}\hat{\mathbf{p}}_{0-}+E_{0s}\hat{\mathbf{s}}\ . \tag{3b}$$

We take the normal to the surface to be the $\hat{\mathbf{z}}$ direction and the wave-vector component perpendicular to $\hat{\mathbf{z}}$ as $\boldsymbol{\kappa}=\hat{\boldsymbol{\kappa}}\,|\,\boldsymbol{\nu}_0\,|\sin\theta_0$. In terms of these, the two polarization directions are

$$\hat{\mathbf{s}}=\hat{\boldsymbol{\kappa}}\times\hat{\mathbf{z}}\ ,$$

$$\hat{\mathbf{p}}_{0-}=\frac{\kappa\hat{\mathbf{z}}+w_0\hat{\boldsymbol{\kappa}}}{\tilde{\omega}} \tag{3c}$$

and the wave vector for the incident field is

$$\boldsymbol{\nu}_{0-}=\boldsymbol{\kappa}-w_0\hat{\mathbf{z}}\ . \tag{3d}$$

The components of the incident wave vector normal (w_0) and parallel (κ) to the medium surface are related by

$$w_0=(\tilde{\omega}^2-\kappa^2)^{1/2}\ , \tag{3e}$$

where $\tilde{\omega}=\omega/c$. In a medium of dielectric constant $\epsilon(\omega)$, the transmitted field is given by

$$\mathbf{E}(\mathbf{r},t)=\mathbf{E}e^{i\boldsymbol{\nu}_-\cdot\mathbf{r}-i\omega t}\ , \tag{4a}$$

where the wave vector in the medium is given by

$$\boldsymbol{\nu}_-=\boldsymbol{\kappa}-w\hat{\mathbf{z}} \tag{4b}$$

and

$$w=(\tilde{\omega}^2\epsilon(\omega)-\kappa^2)^{1/2}\ . \tag{4c}$$

In Eq. (4c) we choose the root with $\mathrm{Im}(w)\geq 0$, and if $\mathrm{Im}(w)=0$, we take $\mathrm{Re}(\omega)\geq 0$. The field in the medium can be obtained from the incident field from

$$\mathbf{E}=\overleftrightarrow{t}\cdot\mathbf{E}_0\ , \tag{4d}$$

where $\overleftrightarrow{t}$ is the Fresnel transmission tensor, given in dyadic notation by

$$\overleftrightarrow{t}=\hat{\mathbf{s}}\hat{\mathbf{s}}t_s+\hat{\mathbf{p}}_-\hat{\mathbf{p}}_{0-}t_p\ . \tag{4e}$$

Here, t_s and t_p are the usual Fresnel coefficients for s- and p-polarized light, respectively,

$$t_s=\frac{2w_0}{w_0+w},\quad t_p=\frac{2nw_0}{w_0\epsilon(\omega)+w}\ , \tag{4f}$$

while $\hat{\mathbf{p}}_-$ is the direction of p-polarized light in the medium given by

$$\hat{\mathbf{p}}_-=\frac{\kappa\hat{\mathbf{z}}+w\hat{\boldsymbol{\kappa}}}{n\tilde{\omega}}=f_s\hat{\mathbf{z}}+f_c\hat{\boldsymbol{\kappa}} \tag{4g}$$

with $n=\sqrt{\epsilon(\omega)}$ the complex refractive index of the medium. Note that if n were real, f_s and f_c would simply be the sine and cosine of the angle of beam propagation in the medium, respectively. For media with a large index of refraction (e.g., Si,Ge), one will typically have $f_c\simeq 1, f_s\simeq 0$. Inside the medium, therefore we can write

$$\mathbf{E}=\hat{\mathbf{s}}E_s+\hat{\mathbf{p}}_-E_p\ . \tag{4h}$$

We now define a new set of coordinates $(\hat{\mathbf{x}}',\hat{\mathbf{y}}',\hat{\mathbf{z}}')$ for each of the three crystal orientations such that the z axis is perpendicular to each crystal face. For the (111) crystal face, therefore, in terms of the standard crystal axes $(\hat{\mathbf{x}},\hat{\mathbf{y}},\hat{\mathbf{z}})$, we have

$$\begin{aligned}\hat{\mathbf{x}}'&=(\tfrac{2}{3})^{1/2}\hat{\mathbf{x}}-\frac{1}{(6)^{1/2}}(\hat{\mathbf{y}}+\hat{\mathbf{z}})\ ,\\ \hat{\mathbf{y}}'&=\frac{1}{(2)^{1/2}}(\hat{\mathbf{y}}-\hat{\mathbf{z}})\ ,\\ \hat{\mathbf{z}}'&=\frac{1}{(3)^{1/2}}(\hat{\mathbf{x}}+\hat{\mathbf{y}}+\hat{\mathbf{z}})\ ,\end{aligned} \tag{5}$$

where we have chosen this definition so that the new x axis is projected on to the original crystal x axis in the plane of the crystal surface. For the (110) surface we have

$$\begin{aligned}\hat{\mathbf{x}}'&=\frac{1}{(2)^{1/2}}(\hat{\mathbf{y}}-\hat{\mathbf{x}})\ ,\\ \hat{\mathbf{y}}'&=\hat{\mathbf{z}}\ ,\\ \hat{\mathbf{z}}'&=\frac{1}{(2)^{1/2}}(\hat{\mathbf{x}}+\hat{\mathbf{y}})\ ,\end{aligned} \tag{6}$$

and finally, for the (001) face we simply choose the z axis to lie normal to the surface. For all faces, this leaves us the freedom of orienting $\hat{\mathbf{x}}',\hat{\mathbf{y}}'$ relative to the beam coordinate axes $\hat{\mathbf{s}}$ and $\hat{\boldsymbol{\kappa}}$ [cf. Fig. 1(b)]. We have, for all crystal faces

$$\begin{aligned}\hat{\mathbf{s}}&=\hat{\mathbf{x}}'\sin\phi-\hat{\mathbf{y}}'\cos\phi\ ,\\ \hat{\boldsymbol{\kappa}}&=\hat{\mathbf{x}}'\cos\phi+\hat{\mathbf{y}}'\sin\phi\ ,\end{aligned} \tag{7}$$

where ϕ is the angle between $\hat{\boldsymbol{\kappa}}$ and $\hat{\mathbf{x}}'$, so that we now have a relationship between the crystal coordinate axes and the beam coordinate axes $\hat{\mathbf{s}},\hat{\boldsymbol{\kappa}},\hat{\mathbf{z}}$.

We now consider the transformation characteristics of the tensor Γ_{ijkl} from the crystal to the beam coordinates. The tensor Γ_{ijkl} contains contributions from the isotropic and the anisotropic piece. The isotropic piece is invariant under this transformation, while for the anisotropic piece ($\Gamma^a_{ijkl}=\zeta\delta_{ijkl}$) we note that in the medium, with respect to the final coordinate axes we have

$$\begin{aligned}\nabla_s&=0\ ,\\ \nabla_\kappa&=i\kappa\ ,\\ \nabla_z&=-iw\ ,\end{aligned} \tag{8}$$

and so obtain

$$\begin{aligned}P^{(2\omega)}_{i,anis}&=i(\kappa\Gamma'^a_{il2n}-w\Gamma'^a_{il3n})E'_lE'_n\\ &\equiv i\tilde{\omega}n\zeta M'^a_{iln}E'_lE'_n\ ,\end{aligned} \tag{9}$$

where Γ'^a and E' are Γ^a and E expressed in the beam coordinate axes. The elements M'^a_{iln} are listed in Table I for the various faces. All elements of M'^a_{ijk} are symmetric with respect to permutation of the indices, and all distinct elements not shown in Table I are zero.

Now that the nonlinear source polarization in the medi-

um has been obtained, we can solve for the fields generated at 2ω. Given a source polarization of the form

$$\mathbf{P}^{(2\omega)}(\mathbf{r},t)=\mathbf{P}^{(2\omega)}(z)e^{2i\boldsymbol{\kappa}\cdot\mathbf{R}-2i\omega t}+\text{c.c.} \tag{10}$$

inside the medium, where $\mathbf{R}=(x,y)$, the fields generated by this polarization will be of the form

$$\mathbf{E}^{(2\omega)}(\mathbf{r},t)=\mathbf{E}^{(2\omega)}(z)e^{2i\boldsymbol{\kappa}\cdot\mathbf{R}-2i\omega t}+\text{c.c.}\ . \tag{11}$$

We introduce the analogous equations to Eq. (4), for the harmonic fields, viz.,

$$\begin{aligned}
&\tilde{\Omega}=\frac{2\omega}{c},\quad \mathbf{K}=2\boldsymbol{\kappa},\quad W=[\tilde{\Omega}^2\epsilon(2\omega)-K^2]^{1/2}\ ,\\
&W_0=(\tilde{\Omega}^2-K^2)^{1/2},\quad \hat{\mathbf{P}}_{\pm}=F_s\hat{\mathbf{z}}\mp F_c\hat{\boldsymbol{\kappa}}\ ,\\
&N=\sqrt{\epsilon(2\omega)},\quad F_s=\frac{K}{N\tilde{\Omega}},\ F_c=\frac{W}{N\tilde{\Omega}}\ ,\\
&\hat{\mathbf{P}}_{0\pm}=\frac{K\hat{\mathbf{z}}\mp W_0\hat{\boldsymbol{\kappa}}}{\tilde{\Omega}}\ .
\end{aligned} \tag{12}$$

TABLE I. Elements of M'^{a}_{ijk} for the various faces.

(001) face

$$\begin{aligned}
M'_{111}&=-\tfrac{1}{4}f_s\sin(4\phi)\\
M'_{222}&=\tfrac{1}{4}f_s[\cos(4\phi)+3]\\
M'_{333}&=-f_c\\
M'_{122}&=\tfrac{1}{4}f_s\sin(4\phi)\\
M'_{112}&=\frac{f_s}{4}[1-\cos(4\phi)]
\end{aligned}$$

(110) face

$$\begin{aligned}
M'_{111}&=-\tfrac{1}{4}f_s[\tfrac{3}{4}\sin(4\phi)+\tfrac{1}{2}\sin(2\phi)]\\
M'_{222}&=\tfrac{1}{4}f_s(\tfrac{3}{4}\cos(4\phi)-\cos(2\phi)+\tfrac{9}{4})\\
M'_{333}&=-\tfrac{1}{2}f_c\\
M'_{133}&=\tfrac{1}{4}f_s\sin(2\phi)\\
M'_{122}&=\tfrac{1}{4}f_s[\tfrac{3}{4}\sin(4\phi)-\tfrac{1}{2}\sin(2\phi)]\\
M'_{112}&=-\tfrac{1}{4}f_s[\tfrac{3}{4}\cos(4\phi)-\tfrac{3}{4}]\\
M'_{133}&=\tfrac{1}{4}f_c[\cos(2\phi)-1)\\
M'_{123}&=-\tfrac{1}{4}f_c\sin(2\phi)\\
M'_{233}&=\tfrac{1}{4}f_s[\cos(2\phi)+1]\\
M'_{223}&=-\tfrac{1}{4}f_c[\cos(2\phi)+1]
\end{aligned}$$

(111) face

$$\begin{aligned}
M'_{111}&=\frac{(2)^{1/2}}{6}f_c\sin(3\phi)\\
M'_{222}&=\tfrac{1}{2}f_s-\frac{(2)^{1/2}}{6}f_c\cos(3\phi)\\
M'_{333}&=-\tfrac{1}{3}f_c\\
M'_{122}&=-\frac{(2)^{1/2}}{6}f_c\sin(3\phi)\\
M'_{112}&=\tfrac{1}{6}f_s+\frac{(2)^{1/2}}{6}f_c\cos(3\phi)\\
M'_{113}&=-\tfrac{1}{3}f_c-\frac{(2)^{1/2}}{6}f_s\cos(3\phi)\\
M'_{123}&=\frac{(2)^{1/2}}{6}f_s\sin(3\phi)\\
M'_{233}&=\tfrac{1}{3}f_s\\
M'_{223}&=-\tfrac{1}{3}f_s+\frac{(2)^{1/2}}{6}f_s\cos(3\phi)
\end{aligned}$$

Again, if N were real, F_s and F_c would become the sine and cosine of the angle of propagation of the harmonic beam in the medium. Following Sipe,[13] the fields outside the medium generated with a half-space filled with a polarization of the form (10) are

$$\mathbf{E}^{(2\omega)}(z)=(E_s^{(2\omega)}\hat{\mathbf{s}}+E_p^{(2\omega)}\hat{\mathbf{P}}_{0+})e^{iW_0z} \tag{13}$$

where,

$$\begin{aligned}
E_s^{(2\omega)}&=B_s(\hat{\mathbf{s}}\cdot\mathbf{P}^{2\omega})\ ,\\
E_p^{(2\omega)}&=B_p(\hat{\mathbf{P}}_+\cdot\mathbf{P}^{2\omega})\ .
\end{aligned} \tag{14}$$

The coefficients B_s,B_p are given by

$$\begin{aligned}
B_s&=\frac{-4\pi\tilde{\Omega}^2}{(W+W_0)(W+2w)}\ ,\\
B_p&=\frac{-4\pi\tilde{\Omega}^2N}{[W+W_0\epsilon(2\omega)](W+2w)}\ .
\end{aligned} \tag{15}$$

The components of the fundamental field in the medium, expressed in the beam coordinate axes are

$$\begin{aligned}
&E_s\ ,\\
&E_\kappa=f_cE_p\ ,\\
&E_z=f_sE_p
\end{aligned} \tag{16}$$

and so the generated fields at 2ω outside of the medium for either s- or p-polarized harmonic light (due to the bulk anisotropic source) for the (100) and (111) face become

$$E_{s,p}^{(2\omega)}=A_{s,p}\frac{i\tilde{\Omega}ng_b}{16N}\zeta[a^{s,p}+b_m^{s,p}\sin m\phi+c_m^{s,p}\cos m\phi]\ , \tag{17}$$

and for the (110) face we have

$$E_{s,p}^{(2\omega)}=A_{s,p}\frac{i\tilde{\Omega}ng_b}{16N}\zeta[a^{s,p}+b_2^{s,p}\sin2\phi+c_2^{s,p}\cos2\phi+b_4^{s,p}\sin4\phi+c_4^{s,p}\cos4\phi]\ , \tag{18}$$

where $m=3$ for the (111) face and $m=4$ for the (001) face in Eq. (17). Note that the coefficients in Eqs. (17) and (18) are distinct for all three faces [i.e., $a^{s,p}(111)\neq a^{s,p}(001)$, etc.] and are defined in Table II. All fields appearing on the right-hand side in Tables II and IV–VI are the fundamental fields inside the medium. The remaining quantities in Eqs. (17) and (18) are

$$\begin{aligned}
A_s&=\frac{4\pi\tilde{\Omega}}{W_0+W}\ ,\\
A_p&=\frac{4\pi\tilde{\Omega}N}{W_0\epsilon(2\omega)+W}\ ,\\
g_b&=\frac{2N\tilde{\Omega}}{2w+W}\ .
\end{aligned} \tag{19}$$

The fields from the bulk isotropic source are the same for all crystal faces, and are calculated next. The isotropic nonlinear source polarization is given by

$$\mathbf{P}_{\rm iso}^{(2\omega)}(\mathbf{r})=\gamma\nabla[\mathbf{E}(\mathbf{r})\cdot\mathbf{E}(\mathbf{r})]$$
$$=2i\gamma(\boldsymbol{\kappa}-w\hat{\mathbf{z}})(E_s^2+E_p^2)e^{2i(\boldsymbol{\kappa}\cdot\mathbf{R}-wz)} \quad (20)$$

and therefore the components of the polarization density are

$$\hat{\mathbf{s}}\cdot\mathbf{P}_{\rm iso}^{(2\omega)}=0\ ,$$
$$\hat{\mathbf{z}}\cdot\mathbf{P}_{\rm iso}^{(2\omega)}=-2i\gamma w(E_s^2+E_p^2)\ , \quad (21)$$
$$\hat{\boldsymbol{\kappa}}\cdot\mathbf{P}_{\rm iso}^{(2\omega)}=2i\gamma\kappa(E_s^2+E_p^2)\ .$$

Finally, from Eqs. (13)—(15) we have for the isotropic fields,

$$E_s^{(2\omega)}=0\ ,$$
$$E_p^{(2\omega)}=A_p i\gamma\tilde{\Omega}F_s(E_s^2+E_p^2) \quad (22)$$

which are identical for all three faces.

The total harmonic field is a superposition of the bulk anisotropic and isotropic contributions, as well as the surface contribution. We consider the surface contribution next.

B. Surface contribution

At the surface of a medium, inversion symmetry is clearly broken, and hence a dipolar contribution to SHG can exist. Also, there is a discontinuity in the normal component of the electric field, which gives rise to a large electric field gradient that can generate a sizeable contribution from higher order multipole terms. The latter effect was first considered by Bloembergen *et al.*,[2] and both surface effects have been discussed by Guyot-Sionnest *et al.*,[12] in detail. In our paper, we account for both effects with an effective surface dipole polarization density given by

$$P_i^{s(2\omega)}=\sum_{jk}\Delta_{ijk}^{(2)}E_jE_k\delta(z-z_0^+)\ , \quad (23)$$

where we follow the convention adopted for surface SHG for metals,[14] and evaluate the fields on the right-hand side of the equation inside the surface.

The symmetry of $\Delta_{ijk}^{(2)}$ is determined by the crystal symmetry within the surface dipole sheet. We assume for simplicity that the surface has a simple unreconstructed structure, and thus for a particular face has the same symmetry as the bulk. The atomic structure for the (111) surface of a diamond lattice is shown in Fig. 2. If only the very top layer [the ("●") atoms] is considered, the surface possesses C_{6v} symmetry; however, if additional surface layers are included, there is C_{3v} symmetry. We therefore use C_{3v} symmetry for $\Delta_{ijk}^{(2)}$, for the (111) face. The atomic arrangement for the (001) face is shown in Fig. 3, where it

TABLE II. Coefficients for bulk anisotropic harmonic field.

	(001) face
$E_s^{(2\omega)}$	$a^s=-2f_sf_cE_sE_p$
	$b_4^s=f_s(E_s^2-f_c^2E_p^2)$
	$c_4^s=2f_sf_cE_sE_p$
$E_p^{(2\omega)}$	$a^p=f_s[F_cE_s^2+E_p^2(3F_cf_c^2+4F_sf_sf_c)]$
	$b_4^p=2f_sf_cF_cE_sE_p$
	$c_4^p=f_sF_c(f_c^2E_p^2-E_s^2)$
	(110) face
$E_s^{(2\omega)}$	$a^s=\frac{1}{2}f_sf_cE_sE_p$
	$b_s^2=\frac{1}{2}f_s[E_s^2+(5f_c^2-2f_s^2)E_p^2]$
	$c_2^s=-2f_sf_cE_sE_p$
	$b_4^s=\frac{3}{4}f_s(E_s^2-f_c^2E_p^2)$
	$c_4^s=\frac{3}{2}f_sf_cE_sE_p$
$E_p^{(2\omega)}$	$a^p=(F_sf_c+\frac{3}{4}f_sF_c)E_s^2+(F_sf_c^3+\frac{1}{4}f_sf_c^2F_c+f_s^3F_c)E_p^2$
	$b_2^p=(2F_sf_c^2-3f_sF_cf_c-2F_sf_s^2)E_sE_p$
	$c_2^p=(F_sf_c^3+f_sf_c^2F_c-2F_sf_s^2f_c+f_s^3F_c)E_p^2-F_sf_cE_s^2$
	$b_4^p=\frac{3}{2}f_sf_cF_cE_sE_p$
	$c_4^p=\frac{3}{4}f_sF_c(f_c^2E_p^2-E_s^2)$
	(111) face
$E_s^{(2\omega)}$	$a^s=\frac{4}{3}f_sf_cE_sE_p$
	$b_3^s=\frac{2(2)^{1/2}}{3}f_c[(f_c-2f_s^2)E_p^2-E_s^2]$
	$c_3^s=-\frac{4(2)^{1/2}}{3}[f_c^2-f_s^2]E_sE_p$
$E_p^{(2\omega)}$	$a^p=(\frac{4}{3}F_sf_c+\frac{2}{3}f_sF_c)E_s^2+(\frac{4}{3}F_sf_c-\frac{2}{3}f_sf_c^2F_c-\frac{8}{3}F_sf_s^2f_c+\frac{4}{3}f_s^3F_c)E_p^2$
	$b_3^p=-\frac{4(2)^{1/2}}{3}(F_cf_c^2+F_sf_sf_c-f_s^2F_c)E_sE_p$
	$c_3^p=\frac{2(2)^{1/2}}{3}[(f_cF_c+F_sf_s)E_s^2-(F_cf_c^3-2f_s^2F_cf_c+F_sf_sf_c^2)E_p^2]$

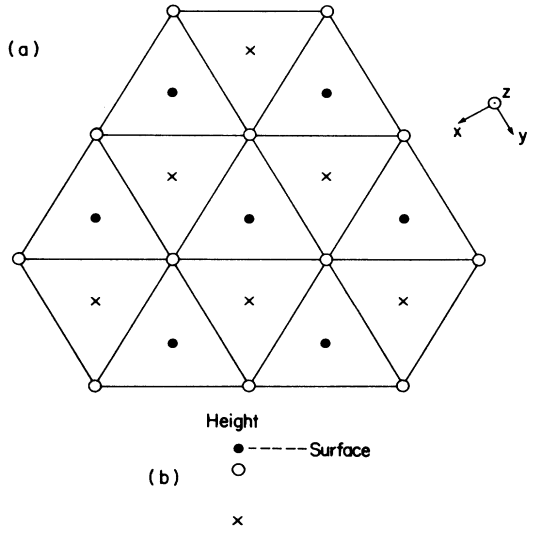

FIG. 2. Atomic arrangement for first 3 layers of a (111) face.

is seen that if one locates the surface on a particular plane [say the ("●") plane] one has C_{2v} symmetry (considering the planes below, as well). However, if one cuts the surface at an adjacent plane of atoms [the "(Δ)" or "(○)" planes], one has C_{2v} symmetry with the mirror plane inclined at 90° to the original plane. In a macroscopic sample, one would expect the surface plane to consist of fractions of all four planes, and hence would exhibit a macroscopic C_{4v} symmetry—the symmetry of a single plane of atoms. For the (110) surface (Fig. 4) we see that the surface in general has only C_s (one mirror plane), symmetry; however, it *is* symmetric with respect to a $\pi/2$ rotation [about the midpoint between "(■)" and "(○)"] and a *vertical* translation of one layer. As in the (100) case, one

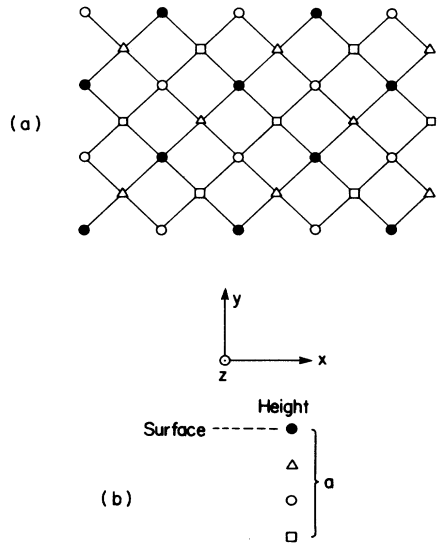

FIG. 3. Atomic arrangement for a (001) surface. Here, a is the conventional unit cell size.

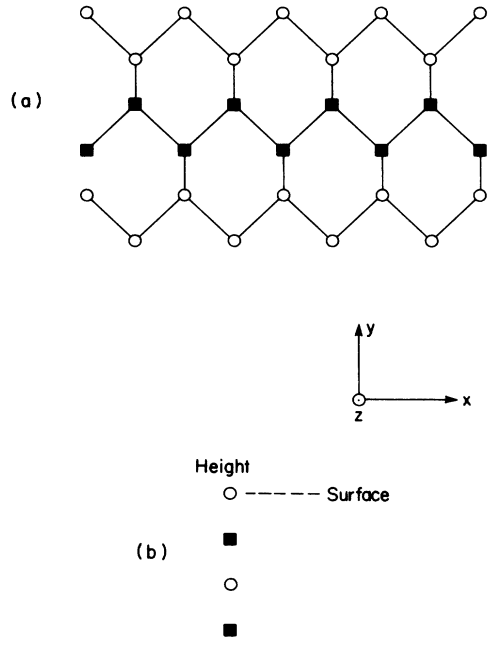

FIG. 4. Atomic arrangements for the (110) surface.

would expect that the surface would contain fractional amounts of both planes on a macroscopic level, and hence would exhibit a macroscopic C_{2v} symmetry.

For the (111) face, with the y axis perpendicular to the plane of symmetry, for C_{3v} symmetry Eq. (23) takes the form[15,16]

$$\begin{bmatrix} P_x^s \\ P_y^s \\ P_z^s \end{bmatrix} = \begin{bmatrix} \partial_{11} & -\partial_{11} & 0 & 0 & \partial_{15} & 0 \\ 0 & 0 & 0 & \partial_{15} & 0 & -\partial_{11} \\ \partial_{31} & \partial_{31} & \partial_{33} & 0 & 0 & 0 \end{bmatrix} \begin{bmatrix} E_x^2 \\ E_y^2 \\ E_z^2 \\ 2E_yE_z \\ 2E_xE_z \\ 2E_xE_y \end{bmatrix}, \tag{24}$$

where ∂_{ij} are constants. Similarly, for the (110) face, the matrix in Eq. (24) becomes[15]

$$\begin{bmatrix} 0 & 0 & 0 & 0 & \partial_{15} & 0 \\ 0 & 0 & 0 & \partial_{24} & 0 & 0 \\ \partial_{31} & \partial_{32} & \partial_{33} & 0 & 0 & 0 \end{bmatrix} \tag{25}$$

and C_{4v} symmetry for a (001) face is obtained by setting $\partial_{31}=\partial_{32}$ and $\partial_{15}=\partial_{24}$. It is important to note that the surface coefficients for various faces are, in general, *not* the same for different faces (i.e., $\partial_{31}^{(100)} \neq \partial_{31}^{(111)}$). If we now express Eqs. (23)—(25) in the beam coordinate axes $(\hat{\mathbf{s}},\hat{\boldsymbol{\kappa}},\hat{\mathbf{z}})$, then we can write the elements $\Delta_{ijk}^{(2)'}$ from Eq. (23) (in the beam coordinates) in terms of the ∂_{ij} in Eqs. (24) and (25) for all three faces. The terms are shown in Table III, where $\Delta_{ijk}^{(2)'}$ is symmetric with respect to $j \leftrightarrow k$, and all distinct elements not shown are zero.

TABLE III. Surface tensor elements.

	(100) face
C_{4v} Symmetry	
	$\Delta'_{113}=\Delta'_{223}=\partial_{15}$
	$\Delta'_{311}=\Delta'_{322}=\partial_{31}$
	$\Delta'_{333}=\partial_{33}$
	(110) face
C_{2v} Symmetry	
	$\Delta'_{113}=\frac{1}{2}(\partial_{15}+\partial_{24})-\frac{1}{2}(\partial_{15}-\partial_{24})\cos(2\phi)$
	$\Delta'_{123}=\Delta'_{213}=\frac{1}{2}(\partial_{15}-\partial_{24})\sin(2\phi)$
	$\Delta'_{223}=\frac{1}{2}(\partial_{15}+\partial_{24})+\frac{1}{2}(\partial_{15}-\partial_{24})\cos(2\phi)$
	$\Delta'_{311}=\frac{1}{2}(\partial_{31}+\partial_{32})-\frac{1}{2}(\partial_{31}-\partial_{32})\cos(2\phi)$
	$\Delta'_{322}=\frac{1}{2}(\partial_{31}+\partial_{32})+\frac{1}{2}(\partial_{31}-\partial_{32})\cos(2\phi)$
	$\Delta'_{312}=\frac{1}{2}(\partial_{31}-\partial_{32})\sin(2\phi)$
	$\Delta'_{333}=\partial_{33}$
	(111) face
C_{3v} Symmetry	
	$\Delta'_{111}=-\partial_{11}\sin(3\phi)=-\Delta'_{122}=-\Delta'_{212}$
	$\Delta'_{112}=-\partial_{11}\cos(3\phi)$
	$\Delta'_{131}=\partial_{15}$
	$\Delta'_{211}=-\Delta'_{222}=-\partial_{11}\cos(3\phi)$
	$\Delta'_{233}=\partial_{15}$
	$\Delta'_{311}=\partial_{31}=\Delta'_{322}$
	$\Delta'_{333}=\partial_{33}$

Following Sipe,[13] the fields in vacuum generated by a source polarization of the form

$$\mathbf{P}^{(2\omega)}(\mathbf{r},t)=\mathbf{\Pi}^{(2\omega)}\delta(z-z_0^+)e^{2i(\kappa\cdot\mathbf{R}-\omega t)}+\text{c.c.} \tag{26}$$

are obtained by assuming the source polarization to be just above the medium surface, and adding the upward second-harmonic wave with the downward second-harmonic wave reflected from the surface of the medium, and are

$$E_s^{(2\omega)}=A_s(i\tilde{\Omega}\hat{\mathbf{s}}\cdot\mathbf{\Pi}^{2\omega}) , \tag{27}$$

$$E_p^{(2\omega)}=A_p[i\tilde{\Omega}\epsilon(2\omega)F_s\hat{\mathbf{z}}\cdot\mathbf{\Pi}^{2\omega}-i\tilde{\Omega}F_c\hat{\boldsymbol{\kappa}}\cdot\mathbf{\Pi}^{2\omega}] . \tag{28}$$

Therefore, combining Eqs. (24)—(28), we have for s- or p-polarized second-harmonic fields generated from the surface of a (111) crystal face,

$$E_{s,p}^{(2\omega)}=A_{s,p}i\tilde{\Omega}[\bar{a}^{s,p}+\bar{b}_3^{s,p}\sin(3\phi)+\bar{c}_3^{s,p}\cos(3\phi)] \tag{29}$$

and for the (001) surface,

$$E_{s,p}^{(2\omega)}=A_{s,p}i\tilde{\Omega}\bar{a}^{s,p} , \tag{30}$$

and finally, for the (110) crystal face, we have

$$E_{s,p}^{(2\omega)}=A_{s,p}i\tilde{\Omega}[\bar{a}^{s,p}+\bar{b}_2^{s,p}\sin(2\phi)+\bar{c}_2^{s,p}\cos(2\phi)] , \tag{31}$$

where the coefficients are listed in Table IV for all faces, and A_s, A_p are defined in Eq. (19). The *total* second-harmonic fields, (bulk and surface isotropic and anisotropic contributions) for either an s- or p-polarized pump beam, from a (100) or (111) crystal face, are then found from

$$\begin{aligned}
\frac{E^{(2\omega)}(||,||)}{E_p^2A_p}&=a_{||,||}+c_{||,||}^{(m)}\cos(m\phi) ,\\
\frac{E^{(2\omega)}(\perp,||)}{E_s^2A_p}&=a_{\perp,||}+c_{\perp,||}^{(m)}\cos(m\phi) ,\\
\frac{E^{(2\omega)}(||,\perp)}{E_p^2A_s}&=b_{||,\perp}^{(m)}\sin(m\phi) ,\\
\frac{E^{(2\omega)}(\perp,\perp)}{E_s^2A_s}&=b_{\perp,\perp}^{(m)}\sin(m\phi) ,
\end{aligned} \tag{32}$$

where, for example $(||,\perp)$ refers to (fundamental, second harmonic) beam polarizations for $p(||)$ and $s(\perp)$ polarized light, respectively, and $m=3$ for the (111) face and $m=4$ for the (001) face. For the (110) face we have

$$\begin{aligned}
\frac{E^{(2\omega)}(||,||)}{E_p^2A_p}&=a_{||,||}+c_{||,||}^{(2)}\cos(2\phi)+c_{||,||}^{(4)}\cos(4\phi) ,\\
\frac{E^{(2\omega)}(\perp,||)}{E_s^2A_p}&=a_{\perp,||}+c_{\perp,||}^{(2)}\cos(2\phi)+c_{\perp,||}^{(4)}\cos(4\phi) ,\\
\frac{E^{(2\omega)}(||,\perp)}{E_p^2A_s}&=b_{||,\perp}^{(2)}\sin(2\phi)+b_{||,\perp}^{(4)}\sin(4\phi) ,\\
\frac{E^{(2\omega)}(\perp,\perp)}{E_s^2A_s}&=b_{\perp,\perp}[\sin(2\phi)+\tfrac{3}{2}\sin(4\phi)] ,
\end{aligned} \tag{33}$$

and the coefficients for all faces are listed in Table V. The forms of the expressions in Eqs, (32) and (33) are consistent with all the experimental data reported to date by various research groups.[1,6,7] In Sec. IV we will consider

TABLE IV. Coefficients for surface contribution.

(001) face

$$\bar{a}^{\,s}=2\partial_{15}f_sE_sE_p$$
$$\bar{a}^{\,p}=\epsilon(2\omega)\partial_{31}F_sE_s^2+[\epsilon(2\omega)\partial_{31}F_sf_c^2-2\partial_{15}f_sF_cf_c+\epsilon(2\omega)\partial_{33}F_sf_s^2]E_p^2$$

(110) face

$$\bar{a}^{\,s}=(\partial_{15}+\partial_{24})f_sE_sE_p$$
$$\bar{b}^{\,s}_2=(\partial_{15}-\partial_{24})f_sf_cE_p^2$$
$$\bar{c}^{\,s}_2=-(\partial_{15}-\partial_{24})f_sE_pE_s$$
$$\bar{a}^{\,p}=\frac{1}{2}\epsilon(2\omega)(\partial_{31}+\partial_{32})F_sE_s^2$$
$$+[\tfrac{1}{2}\epsilon(2\omega)(\partial_{31}+\partial_{32})F_sf_c^2-(\partial_{15}+\partial_{24})f_sF_cf_c+\epsilon(2\omega)\partial_{33}F_sf_s^2]E_p^2$$
$$\bar{b}^{\,p}_2=[\epsilon(2\omega)(\partial_{31}-\partial_{32})F_sf_c-(\partial_{15}-\partial_{24})f_sF_c]E_sE_p$$
$$\bar{c}^{\,p}_2=-\tfrac{1}{2}\epsilon(2\omega)(\partial_{31}-\partial_{32})F_sE_s^2+[\tfrac{1}{2}\epsilon(2\omega)(\partial_{31}-\partial_{32})F_sf_c^2-(\partial_{15}-\partial_{24})f_sF_cf_c]E_p^2$$

(111) face

$$\bar{a}^{\,s}=2\partial_{15}f_sE_sE_p$$
$$\bar{b}^{\,s}_3=\partial_{11}f_c^2E_p^2-\partial_{11}E_s^2$$
$$\bar{c}^{\,s}_3=-2\partial_{11}f_cE_sE_p$$
$$\bar{a}^{\,p}=\epsilon(2\omega)\partial_{31}F_sE_s^2+[\epsilon(2\omega)\partial_{31}F_sf_c^2-2\partial_{15}f_sF_cf_c+\epsilon(2\omega)\partial_{33}F_sf_s^2]E_p^2$$
$$\bar{b}^{\,p}_3=-2\partial_{11}F_cf_cE_sE_p$$
$$\bar{c}^{\,p}_3=\partial_{11}F_cE_s^2-\partial_{11}F_cf_c^2E_p^2$$

what information, apart from symmetry, can be extracted from SHG experiments in general.

III. THIRD-HARMONIC GENERATION FROM CUBIC CRYSTALS

Theoretical expressions for the third-order nonlinear polarization in a medium were first given by Armstrong *et al.*,[17] and discussed by Bloembergen and Pershan.[18] The purpose of this section is to apply the formalism of the preceding sections to derive the analogous equations for THG in reflection with an emphasis on crystal symmetry and orientational dependence of the THG efficiency.

Since THG is electric-dipole allowed in the bulk, the bulk contribution will in general dominate the surface contribution, because of the much larger (typically $\gtrsim 10^2$) volume of sample contributing to THG. This of course assumes no enhancement effects particular to the surface. We therefore consider only the bulk contribution to THG. Even though coherence lengths in solids can be quite short (<1 μm), the escape depth of the third harmonic is considerably smaller than this for frequencies above the band gap in semiconductors, and so coherence effects will have a correspondingly small effect on THG efficiency.

The symmetry properties of $\chi^{(3)}$ for media with cubic symmetry have been given elsewhere.[8] In the standard cubic crystal coordinates, the third-order polarization is given by

$$P_i^{(3\omega)}=3\chi^{(3)}_{1212}E_i(\mathbf{E}\cdot\mathbf{E})+(\chi^{(3)}_{1111}-3\chi^{(3)}_{1212})E_iE_iE_i$$
$$\equiv B\mathbf{E}_i(\mathbf{E}\cdot\mathbf{E})+(A-B)E_iE_iE_i\ , \tag{34}$$

which provides a definition for the parameters A and B. Again, the fields on the right-hand side of Eq. (34) are the fundamental fields inside the medium. In terms of the parameters A and B, we can define the complex anisotropy parameter

$$\sigma\equiv\frac{B-A}{A}\ , \tag{35}$$

which vanishes for isotropic media, where the polarization is then parallel to the fundamental field. Note that the first term in Eq. (34) is simply a vector multiplied by a constant and hence will show no anisotropy when the crystal is rotated, while the last term is a contraction of a fourth rank tensor with three vectors, and can therefore display anisotropic behavior.

The fields from the isotropic contribution are generated from the first term in Eq. (34), and are calculated using Eq. (13) as in the case for SHG. For all faces they are given by

$$E_s^{(3\omega)}=-A_s\frac{g_{3b}}{2N}B(E_s^2+E_p^2)E_s\ ,$$
$$E_p^{(3\omega)}=-A_p\frac{g_{3b}}{2N}B(E_s^2+E_p^2)E_p(F_sf_s-F_cf_c)\ , \tag{36}$$

where

$$g_{3b}=\frac{2N\tilde{\Omega}}{W+3w},\quad \tilde{\Omega}=3\tilde{\omega}$$

and all other quantities are defined in Eqs. (12) and (19) with all harmonic parameters evaluated at 3ω instead of 2ω.

When we transform the ansotropic components, using the same coordinate axes as for the SHG case, we obtain for the anisotropic s- or p-polarized, third-harmonic fields from the (111) or (001) crystal face:

$$E_{s,p}^{(3\omega)}=-A_{s,p}\frac{g_{3b}}{2N}(A-B)[a^{s,p}+b_m^{s,p}\sin(m\phi)$$
$$+c_m^{s,p}\cos(m\phi)]\ , \tag{37}$$

where $m=3$ for the (111) crystal face and $m=4$ for the (001) crystal face. For the (110) crystal face, we have

$$E_{s,p}^{(3\omega)}=-A_{s,p}\frac{g_{3b}}{2N}(A-B)[a^{s,p}+b_2^{s,p}\sin(2\phi)+c_2^{s,p}\cos(2\phi)+b_4^{s,p}\sin(4\phi)+c_4^{s,p}\cos(4\phi)] \tag{38}$$

and the coefficients for all faces are listed in Table VI.

A case of particular interest, for which experiments have been done[9] in Si, is the (001) face at normal incidence. In this case, we have for the total fields,

$$\begin{aligned}
&\frac{E^{(3\omega)}(||,||)}{E_p^3}=A_0\frac{g_{3b}}{2N}\left[\frac{(A-B)}{4}\cos(4\phi)+\frac{(3A+B)}{4}\right],\\
&\frac{E^{(3\omega)}(\perp,\perp)}{E_s^3}=-\frac{E^{(3\omega)}(||,||)}{E_p^3},\\
&\frac{E^{(3\omega)}(||,\perp)}{E_p^3}=-A_0\frac{g_{3b}}{2N}\frac{(A-B)}{4}\sin(4\phi)=\frac{E^{(3\omega)}(\perp,||)}{E_s^3},
\end{aligned} \tag{39}$$

TABLE V. Coefficients for total fields for second-harmonic generation. $\Gamma=in\tilde{\Omega}^2/8(2w+W)$.

(100) face

$$\begin{aligned}
&a_{||,||}=\zeta\Gamma f_s\{3F_cf_c^2+4F_sf_sf_c\}+i\tilde{\Omega}F_s[\epsilon(2\omega)\partial_{31}+\gamma]+i\tilde{\Omega}\epsilon(2\omega)F_sf_s^2(\partial_{33}-\partial_{31})-2i\tilde{\Omega}f_sf_cF_c\partial_{15}\\
&c_{||,||}^{(4)}=\zeta\Gamma f_sF_cf_c^2\\
&a_{\perp,||}=\zeta\Gamma f_sF_c+i\tilde{\Omega}F_s[\epsilon(2\omega)\partial_{31}+\gamma]\\
&c_{\perp,||}^{(4)}=-\zeta\Gamma f_sF_c\\
&b_{||,\perp}^{(4)}=-\zeta\Gamma f_sf_c^2\\
&b_{\perp,\perp}^{(4)}=\zeta\Gamma f_s
\end{aligned}$$

(110) face

$$\begin{aligned}
&a_{||,||}=\zeta\Gamma(F_sf_c^3+\tfrac{1}{4}f_sF_cf_c^2+f_s^3F_c)+i\tilde{\Omega}F_s\left[\epsilon(2\omega)\left[\frac{\partial_{31}+\partial_{32}}{2}\right]+\gamma\right]\\
&\quad+i\tilde{\Omega}\epsilon(2\omega)F_sf_s^2\left[\partial_{33}-\left[\frac{\partial_{31}+\partial_{32}}{2}\right]\right]-2i\tilde{\Omega}f_sf_cF_c\left[\frac{\partial_{15}+\partial_{24}}{2}\right]\\
&c_{||,||}^{(2)}=\zeta\Gamma\{F_sf_c^3+f_sF_cf_c^2-2F_sf_s^2f_c+f_s^3F_c\}\\
&\quad+\epsilon(2\omega)i\tilde{\Omega}F_sf_c^2\left[\frac{\partial_{31}-\partial_{32}}{2}\right]-2i\tilde{\Omega}f_sf_cF_c\left[\frac{\partial_{15}-\partial_{24}}{2}\right]\\
&c_{||,||}^{(4)}=\tfrac{3}{4}\zeta\Gamma f_sF_cf_c^2\\
&a_{\perp,||}=\zeta\Gamma(F_sf_c+\tfrac{3}{4}f_sF_c)+i\tilde{\Omega}F_s\left[\epsilon(2\omega)\left\{\frac{\partial_{31}+\partial_{32}}{2}\right]+\gamma\right]\\
&c_{\perp,||}^{(2)}=-\zeta\Gamma F_sf_c-i\tilde{\Omega}F_s\epsilon(2\omega)\left[\frac{\partial_{31}-\partial_{32}}{2}\right]\\
&c_{\perp,||}^{(4)}=-\tfrac{3}{4}\zeta\Gamma f_sF_c\\
&b_{||,\perp}^{(2)}=\tfrac{1}{2}\zeta\Gamma f_s(5f_c^2-2f_s^2)+i\tilde{\Omega}f_sf_c(\partial_{15}-\partial_{24})\\
&b_{||,\perp}^{(4)}=-\tfrac{3}{4}\zeta\Gamma f_sf_c^2\\
&b_{\perp,\perp}=\tfrac{1}{2}\zeta\Gamma f_s
\end{aligned}$$

(111) face

$$\begin{aligned}
&a_{||,||}=\Gamma\zeta(\tfrac{4}{3}F_sf_c-\tfrac{2}{3}f_sF_cf_c^2-\tfrac{8}{3}F_sf_s^2f_c+\tfrac{4}{3}f_s^3F_c)+i\tilde{\Omega}F_s[\epsilon(2\omega)\partial_{31}+\gamma]\\
&\quad+i\tilde{\Omega}\epsilon(2\omega)F_sf_s^2(\partial_{33}-\partial_{31})-2i\tilde{\Omega}f_sf_cF_c\partial_{15}\\
&c_{||,||}^{(3)}=-\frac{2(2)^{1/2}}{3}\Gamma\zeta(F_cf_c^3-2f_s^2F_cf_c+F_sf_sf_c^2)-i\tilde{\Omega}F_cf_c^2\partial_{11}\\
&a_{\perp,||}=\zeta\frac{2\Gamma}{3}(2F_sf_c+f_sF_c)+i\tilde{\Omega}F_s[\epsilon(2\omega)\partial_{31}+\gamma]\\
&c_{\perp,||}^{(3)}=\zeta\frac{2(2)^{1/2}}{3}\Gamma\{F_cf_c+F_sf_s\}+i\tilde{\Omega}F_c\partial_{11}\\
&b_{||,\perp}^{(3)}=\zeta\frac{2(2)^{1/2}}{3}\Gamma(f_c^2-2f_s^2f_c)+i\tilde{\Omega}f_c^2\partial_{11}\\
&b_{\perp,\perp}^{(3)}=-\zeta\frac{2(2)^{1/2}}{3}\Gamma f_c-i\tilde{\Omega}\partial_{11}
\end{aligned}$$

with

$$A_0 = A_p = A_s = \frac{4\pi}{N+1} ,$$

$$g_{3b} = \frac{2N}{N+n} .$$

The minus sign in the second equation above arises because at normal incidence, the unit vectors for p-polarized light differ in sign for incoming and outgoing waves while for s-polarized light they are the same for both.

IV. SURFACE VERSUS BULK CONTRIBUTIONS

If one intends to use harmonic generation as a probe of crystal bulk or surface structure for centrosymmetric crystals, one must be able to distinguish between surface and bulk contributions. For THG the dominant contribution is from the bulk and THG therefore provides a useful probe of the bulk crystal structure. For SHG however, the surface and bulk contributions can be comparable (by arguments outlined earlier). Guyot-Sionnest *et al.*,[12] have discussed various conditions, within the context of their model for the nonlocal surface contribution, under which the surface contribution is expected to be large relative to the bulk contribution. However, experimentally, one still needs to be able to unambiguously separate the surface and bulk contributions, and it would be useful to accomplish this independent of any model for the surface contribution. We therefore consider the possibility of separating the surface and bulk contributions using only symmetry arguments. For an arbitrary surface face and polarization combination, this task is made difficult by the fact that surface and bulk terms almost always appear together. Hence, any simple variation of the crystal angle ϕ is inadequate to separate the two contributions.

For an isotropic bulk and surface, we have $\partial_{11} = \xi = 0$. In this case, from Eq. (20) it is clear that the bulk polarization is in the ν_- direction and hence will not produce any s-polarized output. From Eqs. (29) and (30) and

TABLE VI. Coefficients for third-harmonic generation.

(001) face

$$a^s = \tfrac{3}{4}(E_s^3 + E_s E_p^2 f_c^2)$$
$$b^s = \tfrac{1}{4} f_c E_p (f_c^2 E_p^2 - 3E_s^2)$$
$$c^s = \tfrac{1}{4}(E_s^3 - 3E_s E_p^2 f_c^2)$$
$$a^p = F_s f_s^3 E_p^3 - \tfrac{3}{4} F_c f_c E_p (f_c^2 E_p^2 + E_s^2)$$
$$b^p = -\frac{F_c}{4}(3E_s f_c^2 E_p^2 - E_s^3)$$
$$c^p = -\frac{F_c f_c}{4} E_p (E_p^2 f_c^2 - 3E_s^2)$$

(110) face

$$a^s = \tfrac{1}{4}\{\tfrac{9}{4}E_s^3 + 3(\tfrac{3}{4}f_c^2 + f_s^2)E_s E_p^2\}$$
$$b_2^s = \tfrac{1}{4} f_c E_p^3 (3f_s^2 - \tfrac{1}{2}f_c^2) - \tfrac{3}{8} f_c E_s^2 E_p$$
$$c_2^s = \tfrac{1}{4} E_s (E_s^2 - 3f_s^2 E_p^2)$$
$$b_4^s = \tfrac{3}{16} E_p f_c (f_c^2 E_p^2 - 3E_s^2)$$
$$c_4^s = \tfrac{3}{16} E_s (E_s^2 - 3f_c^2 E_p^2)$$
$$a^p = \tfrac{1}{4}\{3(F_s f_s - \tfrac{3}{4}F_c f_c)E_p E_s^2 + E_p^3[F_s f_s (2f_s^2 + 3f_c^2) - 3F_c f_c (\tfrac{3}{4}f_c^2 + f_s^2)]\}$$
$$b_2^p = \tfrac{1}{4}[\tfrac{1}{2}F_c E_s^3 + 3(2F_s f_s f_c - F_c f_s^2 + \tfrac{1}{2}F_c f_c^2)E_s E_p^2]$$
$$c_2^p = \tfrac{1}{4}[3E_p^2(F_s f_s f_c^2 + \tfrac{1}{3}F_c f_c^3 - F_c f_c f_s^2) + 3F_s f_s E_p E_s^2]$$
$$b_4^p = \tfrac{3}{16} F_c E_s (E_s^2 - 3f_c^2 E_p^2)$$
$$c_4^p = \tfrac{3}{16} f_c F_c E_p (3E_s^2 - f_c^2 E_p^2)$$

(111) face

$$a^s = \frac{E_s^3}{2} + \left[\frac{f_c^2}{2} + f_s^2\right] E_s E_p^2$$

$$b^s = \frac{-1}{(2)^{1/2}}(f_s E_s^2 E_p - f_s f_c^2 E_p^3)$$

$$c^s = -\sqrt{2} f_s f_c E_s E_p^2$$

$$a^p = F_s \left[E_p^3 f_s \left[\frac{f_s^2}{3} + f_c^2\right] + f_s E_p E_s^2\right] - F_c \left[E_p^3 f_c \left[\frac{f_c^2}{2} + f_s^2\right] + \tfrac{1}{2} f_c E_p E_s^2\right]$$

$$b^p = -\left[F_s \frac{E_s^3}{3(2)^{1/2}} - F_s f_c^2 \frac{E_s E_p^2}{(2)^{1/2}} + F_c f_s f_c \sqrt{2} E_s E_p^2\right]$$

$$c^p = \frac{1}{(2)^{1/2}}\left[\frac{F_s f_c^3}{3} E_p^3 - F_s f_c E_s^2 E_p - F_c f_s f_c^2 E_p^3 + F_c f_s E_s^2 E_p\right]$$

Table IV it is seen that the surface contribution to the s-polarized harmonic beam will then be nonzero only for a mixed s-p input polarization. This enables one to independently measure the $\partial_{15}(=\vec{\chi}^{(s)}_{\|\perp\|})$ coefficient. Alternatively [cf. Eq. (20)], for a circularly polarized pump beam (in the medium) $\mathbf{E}\cdot\mathbf{E}=0$ and hence the γ term vanishes. However, for circularly polarized pump light [cf. Eq. (32) and Table V] all of the surface coefficients contribute to the p-polarized output (the s-polarized output being $\sim\partial_{15}$ as stated). Hence, this approach is not as useful as the first; in addition there is the experimental difficulty of generating circularly polarized light *inside* the medium from non-normally incident light. The first technique has already been applied to surface SHG probe studies of adsorbates on isotropic crystal surfaces.[19]

For cubic materials, however, the anisotropic terms (ζ,∂_{11}) are nonzero. These terms can generate s-polarized output and so the first method of measuring ∂_{15} above, is no longer possible. Therefore, there is apparently no advantage to employing mixed (s,p) polarizations, and so we consider the cases of measuring the s- and p-polarized harmonic beam for either an s- or p-polarized pump beam. For the anisotropic terms, it can be seen from Eq. (32) that by comparing the relative signal sizes from the (111) and (100) faces for s-polarized harmonic output, one can obtain a relative measurement of the quantities

$$|a\zeta|^2 \text{ and } |b\zeta+c\partial_{11}|^2 . \tag{40}$$

where, for a p-polarized pump beam,

$$a=\Gamma f_s f_c^2 ,$$

$$b=\frac{2\sqrt{2}}{3}\Gamma(f_c^2-2f_s^2 f_c) , \tag{41}$$

$$c=i\tilde{\Omega}f_c^2 ,$$

and Γ is defined in Table V. This method was first used by Tom *et al.*[7] for Si at $\lambda=0.53$ μm. Although this method is straightforward, it involves comparing two different samples and is therefore sensitive to differences in surface preparation and structure which may affect the linear fields inside the bulk material. These effects can be monitored with the linear reflectivity; however, the SHG efficiency is much more sensitive to the linear Fresnel coefficients than the linear reflectivity is. In addition, in order to determine the relative magnitudes of ∂_{11} and ζ uniquely, one must measure the relative phase of the second-harmonic signal from the (001) and (111) faces. This is considerably more difficult than measuring the relative magnitude of the signals. To avoid these complications, one might contemplate varying the angle of incidence and looking at the s-polarized output for a (111) surface. If the angular dependence of the functions multiplying ζ and ∂_{11} were significantly different, one would be able to obtain a relative value of ∂_{11} and ζ using measurements made on the same sample. However, as Fig. 5 shows, the variation of SHG with angle of incidence is virtually identical for the two cases of $\partial_{11}=0$ and $\zeta=0$. Hence any attempt to measure ∂_{11} and ζ using this method would seem to be inappropriate.

We consider now the possibility of using the p-polarized output to separate the surface and bulk contributions. Figure 6 shows the SHG efficiency as a function of ϕ [see Fig. 1(b)] for the $(\perp,\|)$ polarization combination from a silicon (001) face, with a fundamental wavelength of $\lambda=0.53$ μm. Shown is a fit to experimental data[20] obtained by setting $|\zeta|\approx\frac{1}{3}|\gamma+\epsilon(2\omega)\partial_{31}|$. The $\partial_{31}(\vec{\chi}^{(s)}_{\perp,\|,\|})$ parameter contains no contribution from the nonlocal response due to the normal field discontinuity. Therefore one might expect[12] that ∂_{31} would be smaller than, or comparable to, γ for silicon or germanium (where the dielectric constants are large). Figure 7 is a plot of the SHG efficiency as a function of ϕ for the $(\perp,\|)$ polarization combination for Si (111) at $\lambda=0.53$ μm. The solid line is a fit to the data,[21] obtained by keeping $|\gamma+\epsilon(2\omega)\partial_{31}|\simeq 3|\zeta|$ as for the (111) face and setting $\partial_{11}=0.18i\zeta$, which is consistent with the result obtained

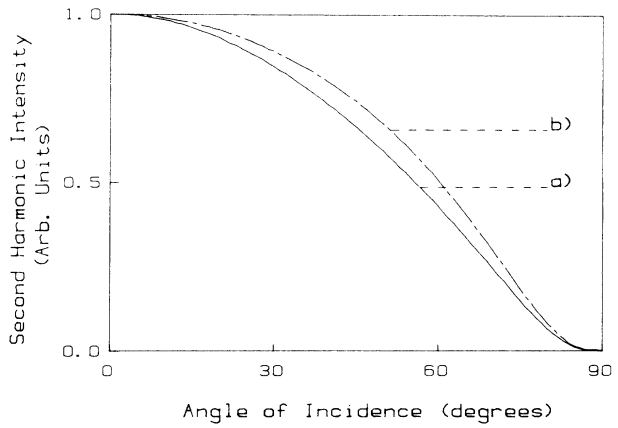

FIG. 5. SHG efficiency of $(\|,\perp)$ polarization combination at $\lambda=1.06$ μm in silicon (111), as a function of angle of incidence. The two curves are for the cases (a) where the ∂_{11} surface parameter is zero and (b) for $\zeta=0$. The vertical scales on both plots have been adjusted to agree at $\theta=0°$.

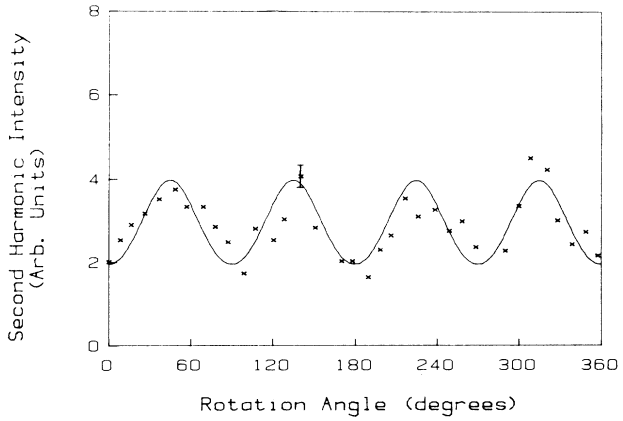

FIG. 6. SHG efficiency versus angle ϕ [see Fig. 1(b)] for Si(100) at $\lambda=0.53$ μm for $(\perp,\|)$ polarization combination. The curve is adjusted to fit the data (crosses) of Ref. 6 by setting $|\zeta|=\frac{1}{3}|\gamma+\epsilon(2\omega)\partial_{31}|$.

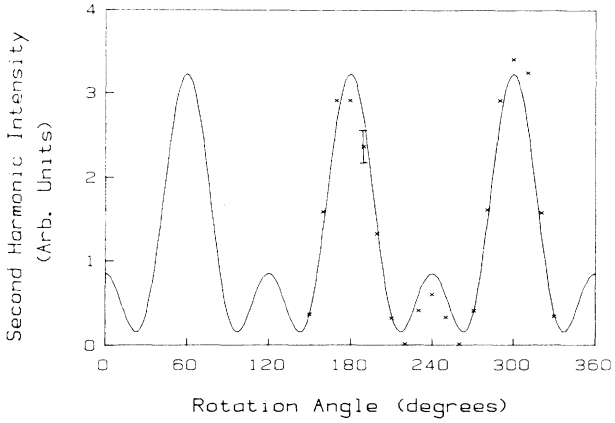

FIG. 7. SHG efficiency versus angle ϕ, for Si(111) at $\lambda=0.53$ μm for $(\perp,\|)$ polarization combination. The data (crosses) are from Ref. 21 and the curve was obtained by keeping $|\zeta| \approx \frac{1}{3}|\gamma+\epsilon(2\omega)\partial_{31}|$ [as for the (100) face] and assuming $\partial_{11}=0.18i\zeta$, consistent with data obtained from Ref. 7.

by Tom *et al.*[7] The fit is reasonably close to experiment, which indicates that ∂_{31} for the two faces are either approximately equal, or more likely that they are small. This result would, of course, be more conclusive if the relative phase between ∂_{11} and ζ were known.

It is well known[1,6,7] that for Si(111) and the $(\|,\|)$ polarization combination, the alternate peaks in the SHG efficiency vanish for a pump wavelength of 0.53 μm, which suggests that for Si(111),

$$|a_{\|,\|}| \sim |c^{(3)}_{\|,\|}| \ . \tag{42}$$

From Table V it is clear that the information contained in Eq. (42) is not particularly useful, since all six nonlinear surface and bulk parameters appear in the equation.

Although experiments have been done[22] using SHG as a time-resolved probe of crystal structure during pulsed-laser melting, these measurements cannot be attributed uniquely to surface or bulk effects since they were performed on a (111) surface. For a (100) crystal face, any anisotropy observed in the SHG efficiency can be attributed solely to the bulk contribution.

In addition to these approaches, one might also consider a multiple-beam experiment as suggested by Guyot-Sionnest *et al.*,[12] to measure the surface anisotropy separately from the bulk anisotropy. Although more complicated, this method would complement measurements of the bulk anisotropic terms via the *s*-polarization output from the (100) face; this approach has perhaps the greatest potential for isolating surface and bulk anisotropies. As discussed by Guyot-Sionnest *et al.*,[12] in cases where surface SHG is performed on samples in high vacuum, various techniques can be employed to verify that the response does indeed arise from the surface contribution (by observing a dramatic decrease in SHG with increasing pressure of oxygen, e.g.). However, for samples in air, these methods are not applicable.

V. CONCLUSIONS

In conclusion, we have constructed a macroscopic phenomenological theory for optical SHG and THG from centrosymmetric cubic crystals based purely on symmetry considerations, and independent of any particular model for the surface contribution to SHG. The form of the expressions for the generated harmonic fields is consistent with all existing data. We considered the possibilities of separating surface and bulk contributions to SHG and found that for cubic crystals, these are very limited. It is therefore concluded that in order to probe bulk crystal properties, THG is a more appropriate means than SHG, whereas for surface studies, optical SHG can, under special circumstances, be used as a surface specific probe.

ACKNOWLEDGMENTS

We gratefully acknowledge financial support of this work from the Natural Sciences and Engineering Research Council of Canada, including additional financial support for D.J.M.

[1]T. A. Driscoll and D. Guidotti, Phys. Rev. B **28**, 1171 (1983); D. Guidotti, T. A. Driscoll, and H. J. Gerritsen, Solid State Commun. **46**, 337 (1983).

[2]N. Bloembergen, R. K. Chang, S. S. Jha, and C. H. Lee, Phys. Rev. **174**, 813 (1968).

[3]C. C. Wang and W. W. Duminski, Phys. Rev. Lett. **20**, 668 (1968); C. C. Wang, Phys. Rev. **178**, 1457 (1969).

[4]T. F. Heinz, C. K. Chen, D. Ricard, and Y. R. Shen, Phys. Rev. Lett. **48**, 478 (1982).

[5]T. F. Heinz, M. M. T. Loy, and W. A. Thompson, Phys. Rev. Lett. **54**, 63 (1985).

[6]J. A. Litwin, J. E. Sipe, and H. M. van Driel, Phys. Rev. B **31**, 5543 (1983).

[7]H. W. K. Tom, T. F. Heinz, and Y. R. Shen, Phys. Rev. Lett. **51**, 1983 (1983).

[8]W. K. Burns and N. Bloembergen, Phys. Rev. B **4**, 3437 (1971).

[9]D. J. Moss, H. M. van Driel, and J. E. Sipe, Appl. Phys. Lett. **48**, 1150 (1986).

[10]C. C. Wang and E. L. Baardsen, Phys. Rev. **185**, 1079 (1969).

[11]H. W. K. Tom and G. D. Aumiller, Phys. Rev. B **33**, 8818 (1986).

[12]P. Guyot-Sionnest, W. Chen, and Y. R. Shen, Phys. Rev. B **33**, 8254 (1986).

[13]J. E. Sipe, J. Opt. Soc. Am. B (unpublished).

[14]J. E. Sipe, V. C. Y. So, M. Fukui, and G. I. Stegeman, Phys. Rev. B **21**, 4389 (1980).

[15]*Handbook of Lasers,* edited by R. J. Pressley (Chemical Rubber Company, Cleveland, 1971), p. 491; M. D. Levenson, *Introduction to Nonlinear Laser Spectroscopy* (Academic, New York, 1982), p. 121.

[16]In the notation in Refs. 7,12, we have

$$\partial_{15}=\chi^{(s)}_{\|\perp\|}, \quad \partial_{31}=\chi^{(s)}_{\perp\|\|}$$

$$\partial_{33}=\chi^{(s)}_{\perp\perp}, \quad \partial_{11}=\chi^{(s)}_{\xi\xi\xi} \ .$$

[17]J. A. Armstrong, N. Bloembergen, J. Ducuing, and P. S.

Pershan, Phys. Rev. **127**, 1918 (1962).
[18]N. Bloembergen and P. S. Pershan, Phys. Rev. **128**, 606 (1962).
[19]T. F. Heinz, Ph.D. Thesis, University of California, 1982.
[20]The data are from Ref. 6. We take this opportunity to correct a typographical error in that paper. Figure 3(a) in that paper is for $\lambda_0=0.53\ \mu$m and Fig. 3(b) is for $\lambda_0=1.06\ \mu$m.
[21]T. A. Driscoll, Ph.D. thesis, Brown University, 1983.
[22]C. V. Shank, R. Yen, and C. Hirlimann, Phys. Rev. Lett. **51**, 900 (1983).